Extinction Conditions of Non-Premixed Flames with Fine Droplets of Water and Water/NaOH Solutions

by

A.K. Lazzarini, R.H. Krauss
and H.K. Chelliah
Department of Mechanical and Aerospace Engineering
University of Virginia
Charlottesville, VA 22903, USA
and
G.T. Linteris
Building and Fire Research Laboratory
National Institute of Standards and Technology
Gaithersburg, MD 20899, USA

NIST CENTENNIAL

NIST
National Institute of Standards and Technology
Technology Administration, U.S. Department of Commerce

EXTINCTION CONDITIONS OF NON-PREMIXED FLAMES WITH FINE DROPLETS OF WATER AND WATER/NaOH SOLUTIONS

A. K. LAZZARINI,[1] R. H. KRAUSS,[1] H. K. CHELLIAH[1] AND G. T. LINTERIS[2]

[1]*Department of Mechanical and Aerospace Engineering*
University of Virginia
Charlottesville, VA 22903, USA
[2]*Building and Fire Research Laboratory*
National Institute of Standards and Technology
Gaithersburg, MD 20899, USA

Interactions of fine droplets of water and water/NaOH solutions with a steady, laminar counterflow methane/air nonpremixed flame are investigated experimentally and numerically. A water atomizer generating a polydisperse distribution of droplet sizes with a median diameter of $20\,\mu$m is used in experiments with steady feed rate. Comparisons of the measured flame extinction condition as a function of droplet mass fraction in the air stream indicate a trend similar to that predicted previously using $20\,\mu$m monodisperse water droplets. The hybrid Eulerian-Lagrangian numerical model previously developed is generalized to include polydisperse distribution of drop sizes; however, the differences seen between experiments and the numerical predictions at high water mass fractions could not be attributed to variation in size distribution alone. Present experiments support the conclusions of an earlier modeling work that on a mass basis, fine water mist can be as effective as the now-banned gaseous fire suppressant halon 1301. Inclusion of NaOH in water (up to 17.5% by mass) is shown to significantly enhance the fire suppression ability of water by complementing its thermal effects with chemical catalytic radical recombination effects of NaOH.

Introduction

On a mass basis, water is known to be a very effective fire suppressant. In particular, water in the form of a fine mist (i.e., drop sizes below $100\,\mu$m), with relatively long settling times under normal gravity conditions, can be an excellent suppressant for gaseous fires in enclosures where total flooding is typically required. Such fires have been previously suppressed using halon 1301, but the production of halon 1301 has been banned because of its adverse effects on the ozone layer [1]. Irrespective of the specific application, detailed quantitative information regarding the fundamental fire suppression mechanism of water mist is useful in order to select types of applications and delivery methods and also to explore methods of enhancing the fire suppression ability of water mist (e.g., through chemical additives). This paper presents such a basic investigation using a counterflow nonpremixed flow configuration, with detailed comparisons between experiments and modeling.

Basic investigations aimed at better understanding the fire suppression mechanism of water dates back to the 1950s [2], while more recent studies have focused primarily on water mist systems [3–8]. Although there is a consensus in the literature on the fundamental fire suppression mechanism of water, no detailed quantitative information on the various physical, thermal, and chemical effects of water mist were available until recent modeling capabilities were developed. The detailed modeling efforts were primarily carried out in two configurations: counterflow [5,6] and co-flow [7]. The former flow configuration provides a convenient approach in understanding the interactions between droplet dynamics with flames, including flame extinction conditions [9–11]. For example, investigations by Lentati and Chelliah [5] have predicted that dilution of the air stream (or displacement of oxygen) with saturated water vapor alone reduces the extinction strain rate of a methane/air non-premixed flame by about 12%. Experimental data are presented for the first time in this paper to support such predictions. Further addition of water, in the form of fine droplets, causes significant thermal cooling of the flame front because of the relatively large latent heat of vaporization of water. For example, addition of 3% of water by mass in the form of $20\,\mu$m droplets (the optimum monodisperse size for this flow configuration) were shown to reduce the extinction strain rate by an additional 55% [5]. By selectively excluding the source terms contributing to the gas phase and the condensed phase conservation equations, the importance of thermal effects associated with water mist were clearly demonstrated [6]. The chemical and other physical effects associated with fine water droplets were shown to have a minor effect.
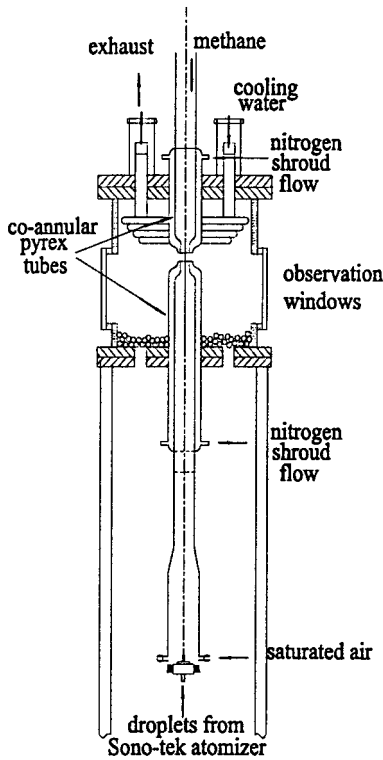
FIG. 1. Schematic of the counterflow burner configuration with the water droplet atomizer.

For a given mass fraction of water in condensed phase, previous predictions with monodisperse size droplets have shown an increase in the flame extinction strain rate when droplet sizes are either below or above 20 μm, indicating a non-monotonic effect on flame suppression as a function of droplet size [5]. Another significant finding in these initial counterflow numerical studies is that on a mass basis, 20 μm water droplets are equally as effective in suppressing counterflow flames as the chemical suppressant halon 1301 [6]. Since these numerical studies were not supported by any experimentation or analytical results, the experiments described here were undertaken to validate such predictions. In practice, however, introduction of monodisperse size droplets at a steady feed rate was found to be a rather difficult task. Although efforts are still underway to achieve this goal, the results presented here used a polydisperse atomizer (described below), for which the size distribution was measured using a phase-Doppler particle analyzer (PDPA) available at the National Institute of Standards and Technology. The previously developed hybrid Eulerian–Lagrangian numerical model [5] for monodisperse water droplet sizes was generalized here to account for such polydisperse size distributions of water droplets. The predicted results with these polydisperse size distributions are shown to be consistent with previous monodisperse predictions; however, differences observed between experiments and modeling could not be explained solely on the basis of the size distribution effects.

In addition to pure water mist results, experimental flame extinction results with water/NaOH solutions are also presented for the present counterflow non-premixed methane/air flame. The significant enhancement in flame suppression ability of water/NaOH solutions (almost a factor of five for 17.5% of NaOH by mass in water) is found to be consistent with previous experiments reported by Zheng et al. [4] for premixed counterflow flames using water/NaCl solutions.

Experimental Method

Counterflow Burner

A steady, planar, nonpremixed flame was established in the mixing layer of counterflowing methane and air streams; Fig. 1 shows a schematic of the counterflow burner. The fuel and air nozzles (Pyrex glass) each have an area contraction ratio of 6.5 and an exit diameter of 1.5 cm, producing nearly plug flow velocity profiles at their exits. Co-flowing nitrogen streams on both fuel and air sides help to maintain a very stable planar flame disk. The nozzles are enclosed in a cylindrical burner chamber, in which water cooling coils and air dilution of the postcombustion gases eliminate secondary flames. The nozzle tubes enter the chamber through vacuum fittings which permit easy adjustment the nozzle separation distance, which is typically set to 12 mm. An air-driven mass flow ejector evacuated the product gases, while a differential pressure gauge records the chamber pressure (typically 12 mm water below atmospheric).

An oil-free shop compressor followed by a series of desiccant beds provides the air, and the fuel gas is methane (BOC grade 4.0, 99.99% purity). Mass flow meters (Teledyne Hastings–Raydist, factory calibrated with a reported accuracy of $\pm 1\%$ of full scale reading) indicate the volumetric flows of the methane and air. For experiments involving water vapor or water droplets, the metered dry air is saturated with water vapor prior to the nozzle exit by bubbling the air through a water bath. A bath heated to 5 °C above ambient produced air stream at the nozzle exit at ambient temperature and 100 $\pm 3\%$ relative humidity (verified with a hygrometer, Testo 605-H1).

The droplet atomizer is located at the base of the bottom (air) tube, and the droplets are entrained in the airflow. The glass tubes allow easy detection of any water condensation on the tube walls. The
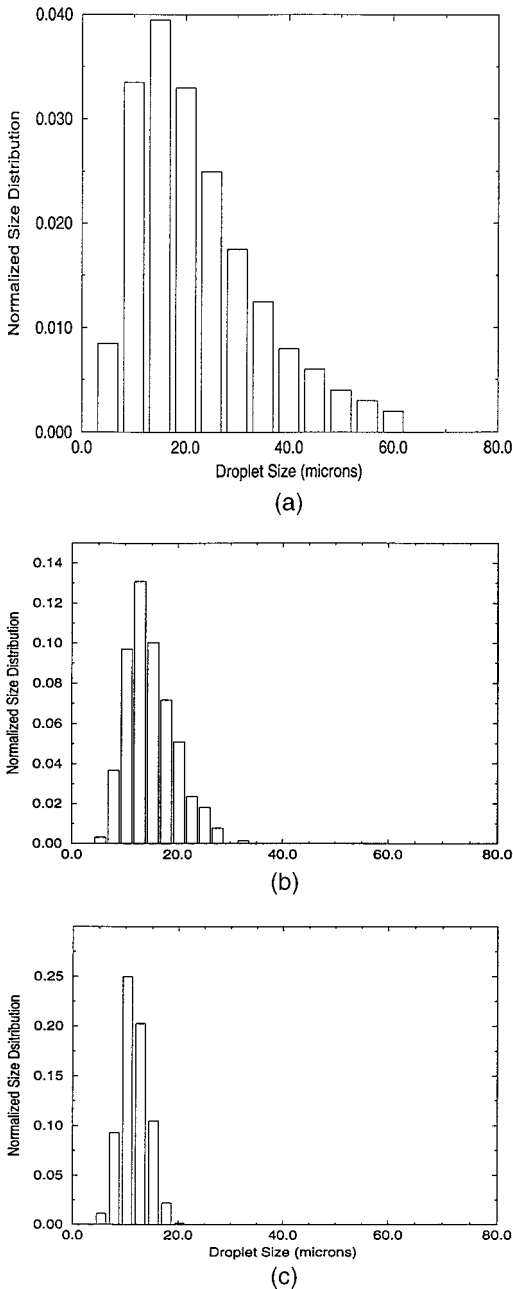
FIG. 2. (a) The normalized droplet size distribution of the Sono-tek atomizer as reported by the manufacturer, divided into 12 discrete sections. (b) The normalized water droplet size distribution measured using a PDPA at the exit of the air nozzle for an airflow rate corresponding to a counterflow strain rate of 285 s^{-1}. (c) The normalized water droplet size distribution measured using a PDPA at the exit of the air nozzle for an airflow rate corresponding to a counterflow strain rate of 160 s^{-1}.

droplet size distribution is measured using a PDPA (Aerometrics, two-component; model, DSA).

Droplet Generation

Two types of droplet generators were tested: (1) a piezoelectrically excited fluid jet atomization system (Fluid Jet Associates) [12] and (2) an ultrasonic fluid surface breakup system (Sono-Tek, Model 8700-120). The first atomizer is capable of generating truly monodisperse droplets (variable by changing the orifice diameter), but the small orifices for our application (10 μm holes generating ~20 μm droplets) proved susceptible to clogging and erosion.

The second atomizer was found to be relatively simple to use and did not clog, but the droplets generated have a much wider size distribution. The median droplet size can be varied by selecting a different length nozzle tip and resonance frequency. All the experimental flame extinction data presented in this paper were obtained using the ultrasonic droplet generator.

The ultrasonic droplet generation system consists of the ultrasonic nozzle and a broadband ultrasonic frequency generator. A syringe pump (Instech Model 2000) with a plastic 10 cc syringe feeds water to the atomizer. In the experiments, the water mass flow rate was fixed, and the air and fuel flows were increased until the flame extinguished. The flame was found to be very stable until the extinction point. The water mass flow at the nozzle exit was measured gravimetrically by carefully collecting all of the saturated air stream (with droplets) and impinging the droplets on a collection surface. These tests showed that while only about 70% of the mass of water injected to the atomizer reached the nozzle exit, the operation of the droplet injection system was very consistent over the entire range of water and air flows of the tests.

Droplet Size Distribution

The droplet number distribution (f) as a function of size (d) in the vicinity of the Sono-Tek atomizer nozzle has been characterized by the manufacturer and is believed to follow a log–normal distribution, given by

$$f(d) = [1/(\sqrt{2\pi}d\sigma)] \times \exp[-(\ln d - \ln \mu)/(2\sigma^2)]$$

with a median diameter (μ) of about 20 μm and a Sauter mean diameter (SMD) of about 30 μm (for $\sigma = 0.6$). This normalized distribution, separated into 12 discrete sections for modeling purposes, is shown in Fig. 2a. Nonetheless, based on the estimated settling velocities of different drop sizes and the flow velocities in the air tube, it is found that not all the drops produced by the atomizer would be convected out of the air nozzle. For example, for an
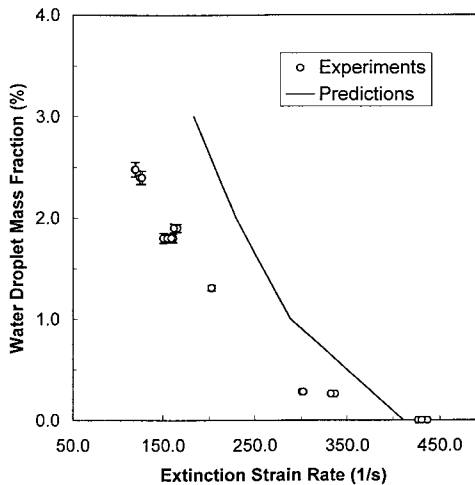
FIG. 3. Variation of water droplet mass fraction in condensed phase as a function of flame extinction strain rate. Symbols are from experiments, and the line is from predictions.

airflow corresponding to a flow strain rate of about 285 s^{-1}, the estimated maximum drop size that could be carried in the air stream was about 75 μm, whereas for a strain rate of 160 s^{-1} the corresponding maximum drop size was about 55 μm. Thus, flow of the droplets generated up the air-nozzle tube would modify the size distribution. We verified this effect through PDPA measurements of the droplet sizes at the air nozzle exit. Fig. 2b shows the measured drop size distribution for a high strain rate of 285 s^{-1}, and Fig. 2c shows a similar plot for a lower strain rate of 160 s^{-1}. While the shift in maximum size of droplets is consistent with our estimates, the general shape of the distribution remains log–normal.

Experimental Extinction Results

With the counterflow burner described above, flame extinction experiments were conducted by increasing the air and methane nozzle exit velocities such that the momentum of the two streams was balanced, that is, $(\rho v^2)_{air} = (\rho v^2)_{CH_4}$, where ρ is the density and v is the axial velocity. Knowing the nozzle separation distance L, the flow strain rate is defined by the global formula $a = 4|v_{air}|/L$ [13]. For non-premixed methane/air flames, the measured global flame extinction strain rate of 470 s^{-1} was obtained, while the measured local flow velocity using a laser Doppler velocimetry system yielded a local flow strain rate of about 390 s^{-1}. Both of these numbers were highly reproducible and consistent with previous experiments and modeling efforts [14]. The experimental flame extinction results presented in

this paper are all based on the global strain rate formula unless otherwise noted.

Water Vapor

The presence of condensed-phase water implies that at equilibrium, the air stream is saturated with water vapor and was verified using a hygrometer. At atmospheric pressure and room temperature of 300 K, the saturated water vapor mole fraction in air is 3.51% (or mass fraction $Y_{vap} = 0.0224$). This saturated water vapor can have a significant effect on the flame extinction condition, mainly through the displacement of oxygen. Previously, detailed modeling efforts have indicated that the predicted local flame extinction strain rate can reduce from 420 s^{-1} for a methane/air flame to 365 s^{-1} for methane and air saturated with water vapor (a reduction in extinction strain of 12%) [5]. Present experiments with saturated water vapor in the air stream have yielded a global extinction strain rate of 405 s^{-1} (i.e., a reduction of 13% from 470 s^{-1} measured for methane and dry air), indicating an excellent agreement with the predictions.

Pure Water Droplets

The ultrasonic atomizer described above (generating droplets of 20 μm medium diameter) is employed here to investigate interactions between water droplets and the non-premixed laminar methane/air flame. With increasing droplet number density (or mass fraction of water droplets in the air stream), it is expected that flame extinction will occur more readily, resulting in a lower extinction strain rate. Fig. 3 indicates such a plot where the mass fraction of water in the condensed phase (Y_0) is plotted as a function of the flame extinction strain rate. Note that the zero water droplet mass fraction corresponds to the case where the air stream is saturated with water vapor (i.e., $Y_{vap} = 0.0224$). In this figure, the symbols are from experiments with the extinction strain rate determined from the global formula. Also shown in Fig. 3 are the predicted variations of water droplet mass fraction as a function of global extinction strain rates, assuming 20 μm monodisperse droplets. Irrespective of the assumption of monodisperse drop size distribution in simulations, the predicted trend is seen to be in reasonable agreement with experiments.

Although the experiments and predictions agree well for pure water vapor, with increasing droplet mass loading the differences become rather large. In predictions, relaxation of the monodisperse size distribution approximation based on the measured distributions shown in Fig. 2 is not expected to rectify this difference because 20 μm monodisperse droplets have been predicted to be the most effective. As discussed later in the numerical section, any broadening of the size distribution about 20 μm leads to
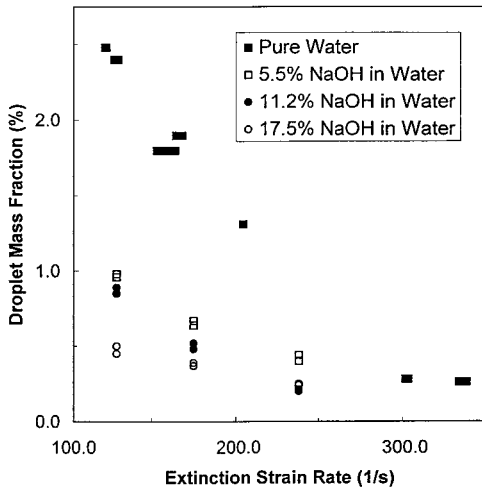
FIG. 4. Comparison of the droplet mass fraction in condensed phase as a function of flame extinction strain rate for different mass loadings of NaOH in water.

Water with NaOH

The primary mechanism of flame extinction by fine water droplets is through the thermal cooling of the flame front, leading to slower chemical reaction rates. For example, in a counterflow field of methane and air, the 20 μm droplets were shown to be most effective because most of the droplet mass is predicted to evaporate near the oxygen consumption or radical species production region [15,16]. This thermal effect of water droplets can be considerably enhanced by including a chemically active fire-suppressing compound in water. NaOH is selected as it known to be the primary compound in the catalytic radical recombination path of sodium bicarbonate fire suppression [17]. Since the solubility of NaOH in cold water is about 30% of the total mass [18], a significant amount of NaOH can be released at the flame front, provided that the fine droplets consisting of water/NaOH are completely vaporized. Here, the same Sono-Tek atomizer generating a median drop size of 20 μm was used to deliver various solutions of water/NaOH and investigate their effect on suppressing counterflow methane/air flames.

Figure 4 shows a plot comparing the experimentally measured water/NaOH mass fractions as a function of the flame extinction strain rate. As before, the air flowing into the nozzle tube was saturated with pure water vapor. Because the NaOH vapor pressure is very small ($<$1 mmHg at room temperature [18]), air saturated with pure water vapor is not expected to affect the evaporation of NaOH. The measured results indicate that with increasing NaOH mass fraction in water, the amount of water/NaOH mass fraction needed for flame extinction decreased significantly—almost a factor of 5 for 17.5% NaOH by mass in water at the lowest strain rate considered. This concept of combining thermal and chemical effects could lead to a significant increase in fire suppression ability, as shown in Fig. 4.

For a selected extinction strain rate, Fig. 4 also shows an interesting nonlinear decrease in total water/NaOH mass fraction with increasing NaOH fraction in the solution. Such a phenomenon may be related to saturation of NaOH in the vapor phase and must be addressed through future modeling efforts.

Numerical Predictions

A hybrid Eulerian-Lagrangian formulation for gas and liquid phases has been employed previously to investigate the dynamics and flame extinction effectiveness of fine water droplets [5]. This model includes a detailed reaction model for methane oxidation and transport of species and energy across the mixing layer. In this approach, knowing the gas-phase solution, the Lagrangian equations for mass, momentum, energy, and particle flux fraction (normalized by that at the air nozzle exit) were integrated in time to determine the droplet location and source terms contributing to the gas-phase conservation equations. With these new source terms, the Eulerian equations describing the gas phase were then integrated using a standard approach [19]. Finally, the two sets of coupled equations were iterated until a predetermined convergence criterion was reached.

Effect of a Constant Mass Flow Rate of Water

As described in the experimental section, the flame extinction was realized by increasing the flow rate of methane and air (saturated with water vapor), while the mass flow rate of condensed water droplets ($\dot{m}_{H_2O,c}$) was held constant by the syringe pump. During this process, the mass fraction of water droplets [$Y_0 = \dot{m}_{H_2O,c}/(\dot{m}_{air} + \dot{m}_{H_2O,c})$] in air changed because of the varying air mass flow rate ($\dot{m}_{air}$). In previous numerical predictions, it was assumed that the condensed phase water mass fraction (Y_0) was held constant at all strain rates. The predicted flame

predicted higher mass fraction of water in the condensed phase for the same flame extinction strain rate. Thus, differences seen in Fig. 3 between experiments and modeling are likely due to other causes. In experiments, calibration of the water droplet mass flow rate through gravimetric analysis can introduce errors; however, considerable care was taken to address uncertainties associated with the approach adopted.
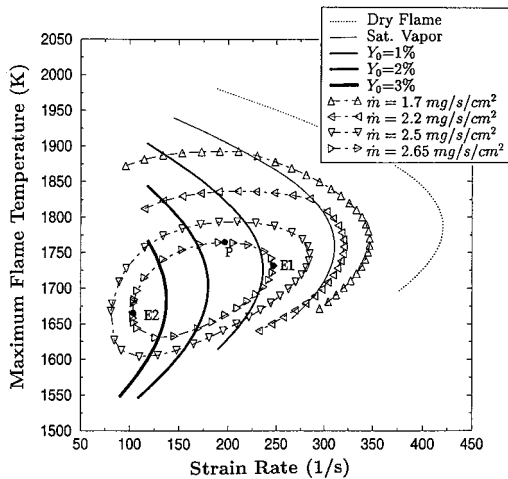
FIG. 5. The variation of the maximum flame temperature as a function of local flow strain rate for constant droplet mass fractions (lines) and constant water mass flux rates (lines with symbols).

temperature variation as a function of flow strain rate for constant $\dot{m}_{H_2O,c}$ and for constant Y_0 are shown in Fig. 5 for 20 μm monodisperse droplets. In the absence of radiative losses, usually only one extinction condition is realized for constant Y_0. Instead, if experiments are performed with constant $\dot{m}_{H_2O,c} = 2.65$ mg/s/cm^2 (innermost closed oval in Fig. 5) and started at some strain rate away from extinction (say point P), then theoretically two flame extinction points can be attained, depending on whether strain rate is increased (point E1) or strain rate is decreased (point E2) by varying only the air and fuel flow rates in a proportional manner to keep the momentum balanced. This phenomenon is purely a consequence of the two-phase system considered, and its occurrence was observed for water/NaOH solutions. In practice, this second extinction point (E2) can be realized by decreasing the oxidizer transport while the droplet transport is held constant.

Effect of Polydisperse Size Distribution

The model developed previously to simulate the interaction of fine water droplets with the counterflow flame assumed monodisperse droplets [5]. This assumption certainly made the computations less demanding, but more importantly, the analyses of the results on droplet size effects became considerably simpler. Because of the experimental difficulties in realizing truly monodisperse water droplets, the above model was generalized here to include the polydisperse size effects. It was shown previously that for water mass loadings similar to those considered here, the ratio of droplet-to-droplet separation distance to droplet size was over 20. Under such conditions, the equation for droplet mass flux ($\mathcal{F}$) (i.e., the spray equation), written in the form for the present quasi-one-dimensional counterflow field [5]

$$\frac{d\mathcal{F}}{dt} + 2\mathcal{F}U_d = \Gamma$$

can be simplified by setting the droplet collision source term $\Gamma = 0$. Thus, by treating the droplet size distribution as composed of several discrete size groups [20,21], the simulation simplifies to solving several Lagrangian equations for these discrete drop size groups, with initial conditions corresponding to each discrete size group specified at the air nozzle exit.

For 1% mass fraction of water in the condensed phase, flame extinction calculations were performed with the three different discrete polydisperse size distributions shown in Fig. 2. A comparison of these flame extinction results with the ideal 20 μm drop size for this flow configuration is shown in Table 1. The predicted extinction strain rates indicate that any broadening of the size distribution of droplets from the ideal 20 μm size leads to a higher flame extinction strain and a further deviation from the experiments. At higher water mass loadings and decreasing flow strain rates, the thermal radiation effects are known to increase and may also have an influence in the present predictions. However, the strain rates indicated in Table 1 are rather moderate, and it is unlikely that the significant differences between experiments and modeling can be solely attributed to radiation heat loss effects.

Conclusions

The main purpose of the present work was to provide experimental data to validate the recent numerical predictions on the effectiveness of fine water

TABLE 1
A comparison between the experimental and predicted global flame extinction strain rate (s^{-1}) for different drop size distributions with the same water droplet mass fraction of 1%

	Experiments	20 μm Monodisperse Droplets	Distribution from Fig. 2a	Distribution from Fig. 2b	Distribution from Fig. 2c
Global strain rate	180	286	297	291	292

droplets in extinguishing counterflow non-premixed flames. On a mass basis, the predicted ability of fine water mist to suppress gaseous fires with similar or better effectiveness than halon 1301 was verified. Although the original goal was to obtain results using monodisperse droplets as assumed in previous theoretical investigations, this task became rather challenging because of difficulties associated with clogging of very small orifices ($\sim$10 μm). Instead, an ultrasonic water atomizer generating log–normal distribution of drop sizes, with a median drop size of about 20 μm, was employed. The actual droplet size distribution was expected to deviate from the prescribed distribution at the atomizer depending on the convective velocity in the air tube in the counterflow burner, and this variation was characterized using a PDPA. The hybrid Eulerian–Lagrangian numerical model was extended to include such polydisperse droplet size distributions, subject to the assumption that the droplet collisions are negligible based on the large separation distance between droplets compared to their diameter.

When the air stream is saturated with water vapor only, it was shown that the counterflow non-premixed flame extinction condition measurements agreed well with the corresponding numerical predictions. With addition of condensed phase water droplets, the trends agreed well; however, considerable differences do exist between the experiments and modeling. The observed differences were shown to be mildly affected by the polydispersivity of the atomizer employed. This led to the conclusion that other submodels in the numerical model, including radiative heat losses, need to be evaluated.

Addition of a chemically active fire-suppressing compound to water, namely NaOH, was shown to complement the thermal fire suppression mechanism of water. At the low end of the strain rates investigated ($\sim$125 s^{-1}), 17.5% by mass of NaOH in the solution was shown to reduce the flame extinction strain rate by almost a factor of five. Although inclusion of NaOH may not be desired in many practical applications because of its corrosive effects, the concept of combining the thermal and chemical effects of these condensed phase agents may lead to the development of superior fire suppressants.

REFERENCES

1. Grosshandler, W. L., Gann, R. G., and Pitts, W. M., *Evaluation of Alternate In-Flight Fire Suppressants for Full-Scale Testing in Aircraft Engine Nacelles and Dry Bays,* NIST SP-861, April, 1994.
2. Rasbash, D. J., Rogowski, Z. W., and Stark, G. W. V., *Combust. Flame* 4:223–234 (1960).
3. Mawhinney, J. R., Dlugogorski, B. Z., and Kim, A. K., *Proceedings of the Fourth International Symposium on Fire Safety Science,* The International Association for Fire Safety Science, 1994 pp. 47–60.
4. Zheng, R., Bray, K. N. C., and Rogg, B., *Combust. Sci. Technol.* 126:389–401 (1997).
5. Lentati, A. M., and Chelliah, H. K., *Combust. Flame* 115:158–179 (1998).
6. Lentati, A. M., and Chelliah, H. K., *Proc. Combust. Inst.* 27:2839 (1998).
7. Prasad, K., Li, C., Kailasanath, K., Ndubizu, C., Ananth, R., and Tatem, P., *Combust. Sci. Technol.* 132:325–364 (1998).
8. Zegers, E. J. P., Williams, B. A., Sheinson, R. S., and Fleming, J. W., "Water Mist Suppression of Non-premixed Counterflow Flames," Eastern States Section Meeting of the Combustion Institute, Raleigh, NC, October, 1999.
9. Continillo, G., and Sirignano, W. A., *Combust. Flame* 81:325 (1990).
10. Lacas, F., Darabiha, N., Versaevel, P., Rolon, J. C., and Candel, S., *Proc. Combust. Inst.* 24:1523 (1992).
11. Chen, N.-H., Rogg, B., and Bray, K. N. C., *Proc. Combust. Inst.* 24:1513 (1992).
12. Takahashi, F., Schmoll, W. J., and Dressler, J. L., *Rev. Sci. Instrum.* 65(11):3563–3569 (1994).
13. Seshadri, K., and Williams, F. A., *Int. J. Heat Mass Transfer* 21:251 (1978).
14. Chelliah, H. K, Law, C. K., Ueda, T., Smooke, M. D., and Williams, F. A., *Proc. Combust. Inst.* 23:503 (1990).
15. Seshadri, K., and Peters, N., *Combust. Flame* 73:23 (1988).
16. Chelliah, H. K., and Williams, F. A., *Combust. Flame* 60:17 (1990).
17. Jensen, D. E., and Jones, G. A., *J. Chem. Soc., Faraday Trans. 1* 78:2843 (1982).
18. Weast, R. C., Astle, M. J, and Beyer, W. H., *CRC Handbook of Chemistry and Physics, 65th ed.,* CRC Press, Boca Raton, FL, 1985.
19. Smooke, M. D., *J. Comput. Phys.* 48:72 (1982).
20. Greenberg, J. B., Silverman, I., and Tambour, Y., *Combust. Flame* 93:90–96 (1993).
21. D'Angelo, Y., Silverman, I., Gao, L. P., Gomez, A., and Smooke, M. D., "Computational and Experimental Study of Counterflow Spray Diffusional Flames," Eastern States Section Meeting of the Combustion Institute, Hilton Head, SC, December, 1996.